Constraining the atmospheric limb of the plastic cycle

Janice Brahney[a,2,1], Natalie Mahowald[b,2,1], Marje Prank[b,c], Gavin Cornwell[d], Zbigniew Klimont[e], Hitoshi Matsui[f], and Kimberly Ann Prather[g,h]

[a]Department of Watershed Sciences, Utah State University, Logan, UT 84322; [b]Department of Earth and Atmospheric Sciences, Atkinson Center for Sustainability, Cornell University, Ithaca, NY 14853; [c]Department of Climate System Research, Climate System Modelling Group, Finnish Meteorological Institute, Helsinki, 00560, Finland; [d]Pollution Management Group, Pacific Northwest National Laboratory, Richland, WA 99352; [e]Energy, Climate and Environment Program, International Institute for Applied Systems Analysis, 2361 Laxenburg, Austria; [f]Graduate School of Environmental Studies, Nagoya University, Nagoya 4648601, Japan; [g]Scripps Institution of Oceanography, University of California San Diego, La Jolla, CA 92093; and [h]Department of Chemistry and Biochemistry, University of California San Diego, La Jolla, CA 92093

Edited by Akkihebbal R. Ravishankara, Colorado State University, Fort Collins, CO, and approved February 16, 2021 (received for review October 8, 2020)

Plastic pollution is one of the most pressing environmental and social issues of the 21st century. Recent work has highlighted the atmosphere's role in transporting microplastics to remote locations [S. Allen et al., *Nat. Geosci.* 12, 339 (2019) and J. Brahney, M. Hallerud, E. Heim, M. Hahnenberger, S. Sukumaran, *Science* 368, 1257–1260 (2020)]. Here, we use in situ observations of microplastic deposition combined with an atmospheric transport model and optimal estimation techniques to test hypotheses of the most likely sources of atmospheric plastic. Results suggest that atmospheric microplastics in the western United States are primarily derived from secondary re-emission sources including roads (84%), the ocean (11%), and agricultural soil dust (5%). Using our best estimate of plastic sources and modeled transport pathways, most continents were net importers of plastics from the marine environment, underscoring the cumulative role of legacy pollution in the atmospheric burden of plastic. This effort uses high-resolution spatial and temporal deposition data along with several hypothesized emission sources to constrain atmospheric plastic. Akin to global biogeochemical cycles, plastics now spiral around the globe with distinct atmospheric, oceanic, cryospheric, and terrestrial residence times. Though advancements have been made in the manufacture of biodegradable polymers, our data suggest that extant nonbiodegradable polymers will continue to cycle through the earth's systems. Due to limited observations and understanding of the source processes, there remain large uncertainties in the transport, deposition, and source attribution of microplastics. Thus, we prioritize future research directions for understanding the plastic cycle.

microplastic pollution | plastic cycle | atmospheric microplastics | plastic aerosols | plastic deposition

Humans have been generating synthetic polymers or "plastics" since the early 1900s, and annual production rates have increased exponentially over the last 70 y. To date, nearly 10 billion metric tons (10,000 Mt or 10 Pg) of plastic have been produced globally (1). Though much of this waste is buried in landfills, recycled, or incinerated, an estimated 12 to 18% of plastic waste ends up in the environment through inadequate management and littering (1–3). Due to their resilience and synthetic nature, plastics do not appreciably decompose; rather, they continually fragment into smaller and smaller pieces. This trait combined with the explosive growth in mismanaged plastics suggests that the mass of accumulated mismanaged plastics may be increasing at a rate of 2- to 10-fold on the decadal time scale (2, 4–6).

Though research is still limited, microplastics in the environment influence soil processes and plant production (7–9), alter microbial community composition (10–12), are consumed by biota leading to impaired health and mortality (13), transfer up the food chain (14), and act as vectors for contaminants (15, 16). Microplastics and their associated contaminants are inevitably consumed by humans, which may lead to adverse health effects (17, 18). Given these preliminary findings, the accumulation and transport of microplastics in the natural environment may have negative and as yet unknown consequences for ecosystems and human health. As plastics make up an increasing fraction of our soils, surface waters, biota, and atmosphere, quantifying the environmental transport processes, rates, and residence times in ways that are analogous to global biogeochemical cycles is necessary to constrain the global plastic cycle (19–21).

While the role of the ocean and riverine systems in accumulating and transporting microplastics has been recognized (2, 22), recent studies have highlighted the importance of the atmosphere as a transporter and reservoir of plastics (23, 24). Remote deposition rates recorded from around the world range from 50 to 700 plastics $m^{-2} \cdot d^{-1}$ (23–29). Based on available data, some 22 Gg (22,000 tons) of microplastic are potentially deposited across the contiguous United States each year (23). These studies have generated numerous questions regarding the plastic cycle. How are plastics emitted to the atmosphere? What are the main sources? Where can we expect to find hot spots of microplastic deposition? How long do plastics remain aloft? Given the current rate of plastic deposition, what can we expect in the future?

At present, it is unclear how plastics are emitted to the atmosphere. Unlike smaller atmospheric particles (<2.5 μm) that are emitted directly through combustion or formed in the atmosphere, coarse mode particles (>2.5 μm) are typically entrained into the atmosphere through mechanical processes, such as dust entrainment during strong wind events or wind or wave breaking of sea surface spray (30). It is reasonable to hypothesize that plastic

Significance

Microplastic particles and fibers generated from the breakdown of mismanaged waste are now so prevalent that they cycle through the earth in a manner akin to global biogeochemical cycles. In modeling the atmospheric limb of the plastic cycle, we show that most atmospheric plastics are derived from the legacy production of plastics from waste that has continued to build up in the environment. Roads dominated the sources of microplastics to the western United States, followed by marine, agriculture, and dust emissions generated downwind of population centers. At the current rate of increase of plastic production (~4% per year), understanding the sources and consequences of microplastics in the atmosphere should be a priority.

Author contributions: J.B. and N.M. designed research; J.B., N.M., and M.P. performed research; N.M., M.P., and H.M. contributed new reagents/analytic tools; J.B., N.M., and M.P. analyzed data; J.B., N.M., M.P., G.C., Z.K., H.M., and K.A.P. contributed ideas for plastic sources; and J.B., N.M., and M.P. wrote the paper with contributions from all authors.

The authors declare no competing interest.

This article is a PNAS Direct Submission.

[1]To whom correspondence may be addressed. Email: janice.brahney@usu.edu or mahowald@cornell.edu.

[2]J.B. and N.M. contributed equally to this work.

This article contains supporting information online at https://www.pnas.org/lookup/suppl/doi:10.1073/pnas.2020719118/-/DCSupplemental.

Published April 12, 2021.

emissions may occur around population centers, where available data indicate relatively high plastic deposition rates (27–29). However, back-trajectory analyses have shown that only a small portion (10 and 25%) of total plastic deposition to remote locations is attributable to direct emissions from population centers (23). Notably, most of the deposited mass was instead related to large-scale atmospheric patterns. In addition to population centers, other less-intuitive sources of atmospheric microplastics are likely.

We postulate that, similar to other coarse mode aerosols, microplastics (<5 mm) are entrained into the atmosphere through mechanical processes, even if this is not the primary source of the plastics to the environment (Fig. 1). For example, concentrated areas of plastics and microplastics in marine environments represent an important potential source of microplastics that can be aerosolized through wind or wave action, similar to sea spray aerosols (22, 31). Insoluble plastic particles tend to be concentrated at the top of the mixed layer due to their low density and upward transport by gas bubbles. Thus, these particles are easier to entrain into wind- or bubble-generated sea spray (32). Secondly, vehicle tires, brakes, and road surfaces contain plastic, which can be worn and generate microplastics that are emitted into the environment (33–36). More importantly, the mechanical process of vehicle tire movement, the braking process, and the intense turbulence in the wakes of vehicles allow these roadside plastics to gain sufficient mechanical energy to overcome inertial or cohesive forces and be resuspended into the atmosphere. A third potential re-emission source of plastics are dusts produced from agricultural fields during tilling or when fallow. Agricultural fields are likely hotspots of soil plastic concentrations for two primary reasons. Approximately 55% of the biosolids produced in US waste treatment operations are applied as fertilizer around the country. This application of biosolids to agricultural fields is also practiced globally (37, 38). Because ~98% of the microplastics in wastewater are retained in biosolids (39), the application of biosolids to agricultural fields represents a significant pathway for microplastics to enter the environment. In addition, plastic mulch is often added to soils to increase temperatures while retaining moisture (40). Fourth, if atmospheric plastic deposition is ubiquitous, microplastics should be found in the soils of most landscapes. Thus, it stands to reason that microplastics can be re-emitted to the atmosphere from soils undergoing wind deflation, especially close to or downwind of population centers (hereafter referred to as "population dust").

To what extent each of these sources may contribute to the atmospheric burden of plastics is not yet clear. Our goal in this study is to combine the limited observations of atmospheric microplastics with models to better identify the open research questions. Here, we use a detailed deposition dataset available for the remote parts of the western United States in combination with a microplastics-enabled version of the Community Atmospheric Model (CAM) (41) to determine the most likely sources of atmospheric microplastics, their residence time in the atmosphere, and their accumulation areas. This very detailed deposition dataset includes temporal and spatial variability in addition to size-resolved count and volume information about plastics, which allow us to uniquely consider the plastics number and mass (23). Both mass and number are important, but here we focus our results on mass to frame our understanding of plastic movement through the earth system and because mass will better reflect the ecological and biogeochemical implications.

The aerodynamic size of plastics is very important for atmospheric residence time but is still poorly understood for fibers and other asymmetric shapes (42, 43). Recognizing that models may overestimate dry deposition rates for large asymmetric particles of well-studied aerosols like dust (42, 43), we simulated transport of particles with aerodynamic diameters ranging from 0.3 to 70 μm and used three different assumptions about the size distribution of the deposited microplastics for our model-data comparison, with our base case being the medium size (Fig. 2*A*). Similar to other relatively large insoluble particles like dust, we assume that plastics can be scavenged in precipitation events, as seen in the observations (23, 44). Note that our observations only cover the diameter size range from 4 to 250 μm, and that is the size range we consider here. The spatial distribution of the sources is fixed and used as the plastic source for the atmospheric modeling of the three-dimensional distribution, transport, and deposition, but the strength and size distribution of the different sources is varied to best match the observations (more details in the *Materials and Methods* section). Errors are based on model-data comparisons for the exact same time period as well as field, laboratory, and process blanks.

Results and Discussion

We estimated that the current average total atmospheric burden (content) of microplastics over the land regions of the western United States is 1 Gg (0.001 Mt) (Fig. 1). The largest contributor to modeled plastic deposition in the western United States is from road dust sources (84%), while ocean emissions contributed 11% of the plastic deposition. Agricultural dust represents plastics entrained into the atmosphere from agricultural fields

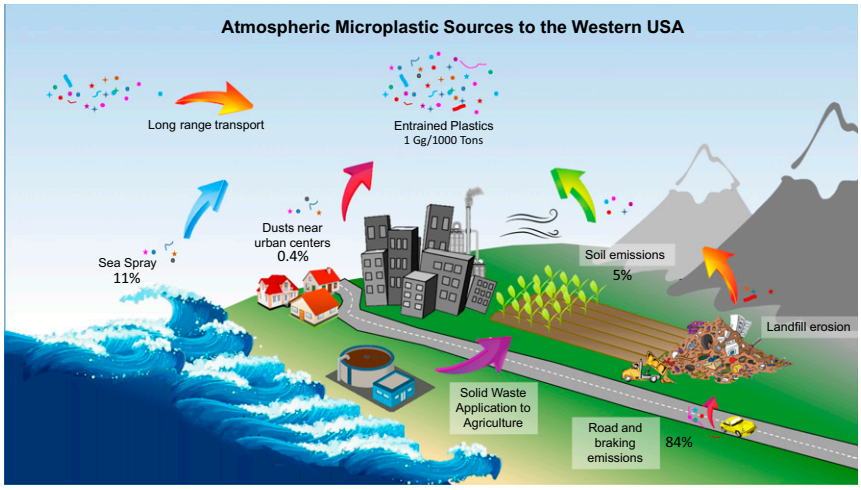

Fig. 1. Representation of the major sources of microplastics to the atmosphere and their relative contributions to deposition to the terrestrial environment over the western United States (30 to 50°N, 120 to 100°W). Over this region, the deposition of microplastics is 84% from roads, 11% from sea spray, 5% from agricultural dust, and 0.4% from dust near population centers. The atmospheric burden above this region is 1 Gg (0.001 Mt).

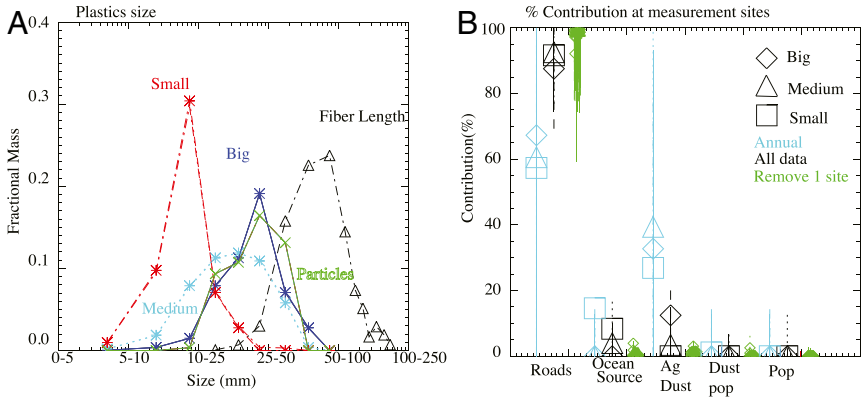

Fig. 2. (*A*) The fractional mass by size of the particles (green x's) and fibers in the observations (black triangles). In the model, the particles are assumed to be transported as observed, but because the fibers are mostly 1 μm in diameter but much longer, the aerodynamic size that is appropriate is not well established and thus are simulated in three sizes: small (red), medium (cyan), and big (dark blue), with medium being the base case. (*B*) Estimates of the contribution at the observing sites from different sources as inferred using the method described in *Materials and Methods* for the three sizes: big (diamond), medium (triangle), and small (square). For all sources and cases, the 95% confidence limits are shown as vertical lines. Multiple sensitivity studies were conducted (see *Materials and Methods* for details) with time averaging (cyan) and with each site withheld (green), showing the ranges of values that can be obtained for each relative source strength.

and contributes 5% of the plastic deposition (Fig. 1). Interestingly, both sources of plastics from population centers, either from dust generated downwind of population sources (population dust) or directly related to population, represent a much smaller contribution (0.3 and 0%, respectively) (Fig. 1).

To better understand the relative plastic source contributions at the observational sites, we report the modeled contribution at the sites over the observed time period (Fig. 2*B*). The road source contributed 92.5% [69 to 100%] of the modeled annual average deposition (the bracketed values represent the 95% confidence limits across the three size cases), while the oceans and agricultural dust sources contributed 4.0 [0 to 17%] and 3.4% [0 to 22%], respectively (Fig. 2*B*). The population dust and the population source contributed 2×10^{-7} [0 to 8%] and 0% [0 to 13%], respectively. Notice that the contribution of plastic sources at our observational sites are slightly different from over the whole western United States (in Fig. 1). This is, in part, because the ocean source tends to be larger closer to the coasts than at our observational sites. The road source has the smallest uncertainty, with a range spanning 30%, while the other sources suggest an uncertainty of 100%, indicating that this first estimate of the relative contributions of sources should be refined in future studies.

A comparison of our model results with the detailed plastic deposition data from the western United States suggests that the model is able to simulate the range of plastic deposition seen at the sites, which provides a measure of confidence in the relative source attributions presented for the western United States (Fig. 3*B*). The model is not able to simulate all the variability in these remote and mountainous regions (Fig. 3*B* and *SI Appendix*, Fig. S1 and Table S1), as it is similarly unable to simulate dust and sea salt aerosols at these sites (*SI Appendix*, Table S2). While remote sites represent our best opportunity to sample air uncompromised by local sources and thus understand the long-range transport of plastics, the complex terrain of mountainous regions make it difficult for models to accurately simulate transport and deposition. The model results showing the relative contribution of different sources to the final model result highlight that the ocean source of plastics is not well constrained by these observations. These stations are distant from the shore, which contributes to the large uncertainty in the ocean source (Fig. 3 *C*–*E*).

The uncertainties in the aerodynamic size of the plastics are important for the modeled uncertainties (contrast the square, triangle, and diamond symbols in Fig. 2*B*), and we include all three size distributions in our 95% estimates above. This suggests that characterizing the aerodynamic behavior of these heterogeneous particles is important for understanding their transport pathways. In addition, the sensitivity studies show that having temporally resolved data improves our constraints on the sources (Fig. 2*B*: cyan symbols and lines are constraints using only annually averaged model-data comparisons at each of the 11 sites). Even more important is having 11 different observing stations; excluding individual stations from the analysis enlarges the 95% confidence limits for all the sources (Fig. 2*B*: green symbols and lines). Thus, more detailed spatial and temporally resolved data are vital for improving our understanding of the long-range transport of microplastics.

Importantly, our data do not include plastics smaller than 4 μm as this fraction has yet to quantified (45), but such particles could have longer residence times than the ones included here (weeks instead of hours). It is not known how important plastics smaller than 4 μm are in the atmosphere, and their behavior needs to be measured and assessed. The data shown here do, however, indicate that particles and fibers decrease in number as they decrease in size (Fig. 2*A*). This suggests that similar to other mechanically generated aerosols (like dust), most of the mass is emitted in larger sizes; for dust, less than 10% of the PM10 (particles less than 10 μm) is emitted in PM1 (particles less than 1 μm) (46, 47). Smaller particles tend to be more difficult to entrain into the atmosphere as they experience stronger cohesive forces and yet have smaller cross-sectional areas exposed to the winds. While this is not the case for the plastics emitted with sea spray, which could theoretically contain small plastics, the locations of the measurement stations far from shore do not allow us to constrain the ocean source well, especially as these small particles would be embedded in larger hygroscopic sea salt particles that would reduce their atmospheric residence time. More in situ and laboratory studies are required to better understand the number and mass of plastics that are emitted in the submicron size fraction.

Next, we consider whether other observations support the inferred sources. Because of the limited data, we extrapolate our study globally for this comparison. Our emission estimates of long-range transported microplastics from tire wear and braking are on the low end of recent bottom-up estimates (here 96 [63 to 110] $\mathrm{Gg \cdot y^{-1}}$ versus 284 (102 to 787) $\mathrm{Gg \cdot y^{-1}}$) (36) (Fig. 4*A*). The range in ref. 36 is associated with assumptions about the fraction of the plastics emitted for long-range transport, which they assume is less than 10 μm. In their model, they used a range of values

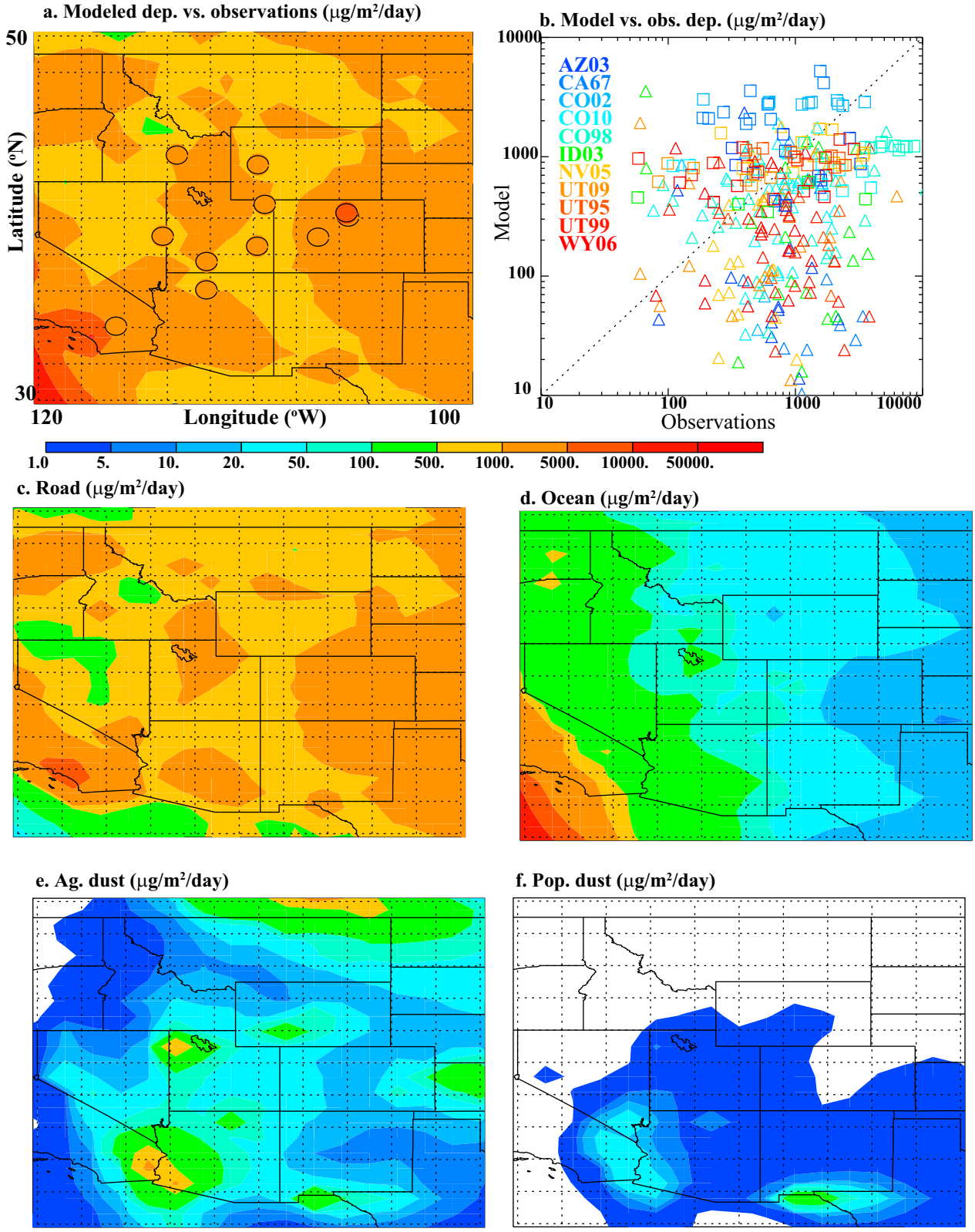

Fig. 3. Model estimates of microplastic deposition using the best estimate (μg/m^2/d). (*A*) Total plastic deposition from all the different model sources and the annual average of the observations at the sites (filled circles). (*B*) A scatterplot of the model versus observations for wet (triangles) and dry (squares) deposition ($r = 0.11$, $n = 313$). The station names are abbreviated from the National Atmospheric Deposition Network, following *SI Appendix*, Table S1, and the latitude and longitude are as follows: AZ03 (36.1°N, 247.8°E), CA67 (34.1°N, 243.6°E), CO02 (40.1°N, 254.4°E), CO10 (39.0°N, 253.0°E), CO98 (40.3°N, 254.4°E), ID03 (43.5°N, 246.5°E), NV05 (39.0°N, 245.8°E), UT09 (38.46°N, 250.2°E), UT95 (40.8°N, 250.5°E), UT99 (37.6°N, 247.8°E), and WY06 (42.9°N, 250.2°E). The total microplastic deposition (*A*) is the sum of the road tire and braking (*C*), ocean (*D*), agricultural dust (*E*), and population dust (*F*), which is the dust generated downstream from population centers. Notice that the population source is not plotted as it is zero in the best estimate.

representing their range of observations (29). Here, in contrast, we constrain this source using the remote observations. Our results suggest that the lower end of their assumption is more likely correct. However, the differences between their bottom-up estimates and our top-down results could be due to errors in our modeling or model-data comparisons, or that emissions may be smaller in the western United States, where our sites are located, compared to Europe, from where the bottom-up estimate derives. For example, in Europe and Asia, there is documented recycling of plastics into the production of road surfaces (35, 48), while this practice is still limited in the United States. The differences could also be due to the small fraction of emitted microplastics that are actually suspended high enough to be entrained in the atmosphere for long-range transport. Concentrations of large particles close to the surface (<2 m) can be one to four orders of magnitude greater than the concentration in the boundary layer that can be transported long-range, as large particles settle rapidly out of the atmosphere (49, 50).

Our modeled spatial distribution of the ocean deposition is driven by the source term for the microplastics, which is driven by a combination of observed microplastic concentrations in gyres, especially the North Pacific and elsewhere that the sea spray source (driven mostly by winds) is strongest in the model [Fig. 4 and *SI Appendix*, Fig. S4 (22), see *Materials and Methods* for more details]. Our assumptions of oceanic microplastic concentrations are based on syntheses of ocean microplastic observations (8). Notice that, in the western United States, the deposition from the ocean source drops off quickly as we move onto land, and by the time we are at the remote mountain stations used for this study, plastic deposition has dropped substantially (Fig. 3*D*). This is because of the short residence time of the plastics in the size range studied here (*SI Appendix*, Table S3). In other words, our results hint that there could be significantly large sources of plastics from oceans (globally perhaps 8.6 [0 to 22] Tg or Mt $\cdot$ y^{-1}, including the 95% confidence limits), but the location of our sites is not ideal to characterize these emissions. Recent studies on the ocean coast in France suggest higher observed marine concentrations as compared to our modeled concentrations of microplastics [observed: ~9 microplastics m^{-3} versus base modeled value of 0.06 microplastics m^{-3} (31)]. However, the observations in France were taken close to the surface and may not be representative of long-range transported plastics. In addition, the mass of plastics required for our source is lower than recent studies have observed in the ocean for a slightly larger size fraction (*SI Appendix*, Fig. S3) (22), suggesting that our estimates of ocean sources may actually be on the low side.

Our estimates of agricultural microplastic emissions with dust over the western United States are ~0.2 Gg per year, and if we extrapolate globally, 69 [0 to 450] Gg $\cdot$ y^{-1}; notice there tends to be greater agricultural dust emissions outside the region where we have data, so this extrapolation requires validation through additional sample collection (*SI Appendix*, Fig. S4*B*). Using satellite data, global emission estimates of long-range transported agricultural dust suggest a source of −34 Tg $\cdot$ y over North America (much of this east of our region) or ~170 Tg $\cdot$ y^{-1} globally (51). Dividing our inferred sources for the plastics from agricultural dust in the western United States and the world by these published estimates of the agricultural dust production, we infer a concentration of microplastics in agricultural soils of 7 to 400 mg $\cdot$ kg^{-1}. Observations range from 0.2 mg $\cdot$ kg^{-1} in areas of the United States where biosolids have not been applied to >2,000 mg $\cdot$ kg^{-1} in areas of China where plastic mulching is commonly used (52–56), indicating our agricultural microplastics sources are within the large range of reported values.

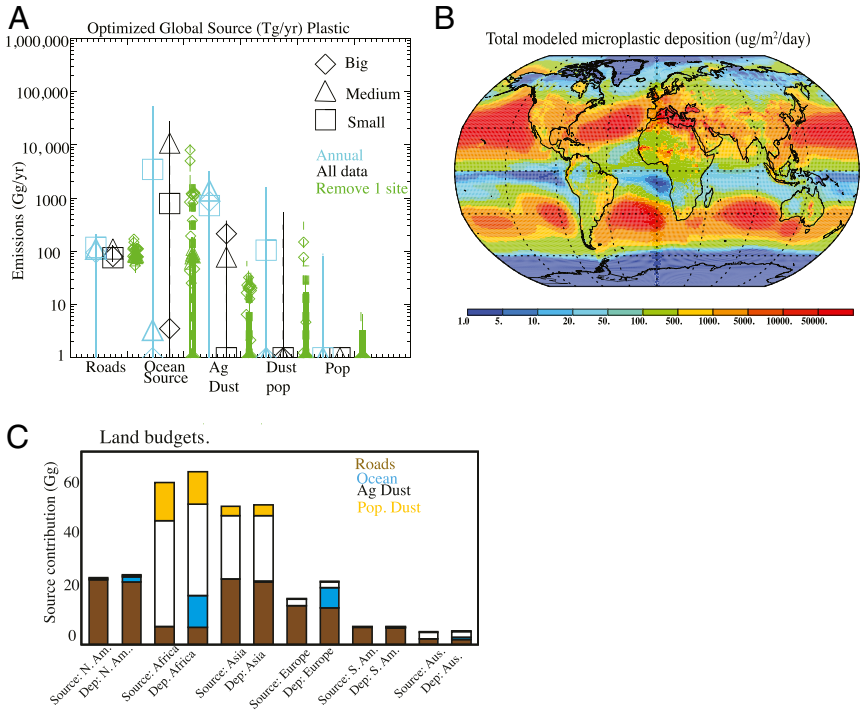

Fig. 4. Globally averaged sources of microplastics (*A*) as inferred using the methods described in *Materials and Methods* for the three size ranges: big (diamond), medium (triangle), and small (square). For all sources, the 95% confidence limits are shown as vertical lines. Multiple sensitivity studies were conducted (see *Materials and Methods* for details) with time averaging (cyan) and with each site withheld (green), showing the ranges of values that can be obtained for each source strength extrapolated globally. (*B*) The total microplastic deposition estimated in the model (μg/m^2/day). (*C*) The modeled budgets for different continents in terms of sources and deposition (excluding coastal grid boxes). Roads (brown), ocean (blue), agricultural dust (white), and population dust (yellow) contributions in Gg/y are shown for each continent using the medium size (base case).

Constraints on the strength of the plastic sources downwind of populations (population dust) or directly from population sources are not available in the literature, even though this is where most plastics are used. It is somewhat surprising that population sources were less important in describing our observed spatial and temporal microplastic data. It may be that the modeled distribution of plastics from population centers looks very similar to the tire wear and braking source, but the latter does a better job of simulating the observed distribution. This suggests that, although population centers may provide the initial source of plastics waste, roads provide the mechanical energy to emit these plastics to the atmosphere (33, 34). Plastics emitted directly from population centers could be too large for long-range transport and get deposited nearby, where they can gradually degrade to microscopic sizes due to sunlight exposure, temperature changes, freezing and melting water, and mechanical forces from vehicles.

Hann et al. (57) analyzed the generation and fate of microplastics in the environment from populated areas of the European Union. Sources related to roads (break and tire wear and road markings) made up most of their reported emissions. In addition, they identified several other relevant sources, the largest being losses of preproduction plastic pellets, clothes washing, building paints, and artificial turfs. Plastic pellets come in sizes too large for long-range atmospheric transport. Building paints and artificial turfs could lead to direct atmospheric emissions of microplastics; however, these are likely to only be a small fraction of the emissions as it is hard to get small particles airborne. Emissions of synthetic microfibers to the environment from apparel washing are reported to be up to 350 kt/y globally (58). Emissions from laundry drying have been reported to be several times greater (59) or comparable (60) to the fibers emitted in wastewater. Emissions to the environment from plastic waste recycling may also be similar in magnitude (60). Unfortunately, there is no information available on what fraction of the microplastic from these sources would be small enough for long-range atmospheric transport.

Reported fluxes of mismanaged macroplastic pollution to the environment are much larger than microplastic fluxes, and according to the model of Kawecki and Nowack (60), about two-thirds of mismanaged macroplastic pollution end up on roadsides, where exposures to environmental factors can break it down to microscopic fragments. Thus, by virtue of their proximity to people, roads can effectively accumulate from a variety of sources plastics that are subsequently broken down and emitted high into the atmosphere by traffic. Support for this idea comes from an examination of road dust in the district of Tehran, Iran. The researchers found a diversity in urban microplastic color and character, suggesting most plastics were derived from multiple commodity sources rather than just tire wear (61). Based on this reasoning, it follows that road sources dominated the atmospheric loads to the western United States, even though tire and road wear plastics were rare in the observed samples (23). It is worth noting that most of the sites in the western-US study region are in arid regions (9 of 11 sites), which may increase the potential for road-based emissions as compared to wet regions where surface runoff may migrate microplastics to soils or waterways. More studies on primary plastic sources, environmental fate, and entrainment are required to better constrain this aspect of the plastic cycle.

Implications and Future Work

For this study, we used the most complete observational dataset published of atmospheric plastic deposition, which comes from in the western United States (23). We extrapolated our model to the global level (Fig. 4*A*) to see what additional work needs to be done, which regions should be prioritized for more observations (Fig. 4*B*), and to understand the implications of this study on the global plastic cycle. This extrapolation assumes that similar sources of dry and wet deposition occur globally as compared to those in the western United States and thus should be considered tentative. Comparisons of our model results to the limited available global data suggest that the model results tuned to one dataset in North America may underestimate deposition in Europe, although most of the compared estimated rates are based on deposition data from a limited time period and may not robustly represent long-term microplastic deposition (*SI Appendix*, Fig. S4 and Table S1) (24, 25, 27, 28, 62).

Our study suggests the strongest sources and greatest deposition rates of plastics occur over the ocean (Fig. 4*B*), especially over the Pacific and Mediterranean, which aligns with recent evidence indicating that these waters have 2 to 3× the fiber concentrations of other ocean basins (22, 63); however, even these emissions are poorly constrained by our observational sites (see large uncertainty in Figs. 2*B* and 4*A*, and distribution of modeled deposition from oceans: Fig. 3*D* and *SI Appendix*, Fig. S2). The United States, Europe, Middle East, India, and eastern Asia were hotspots for terrestrial plastic deposition (Fig. 4*B* and *SI Appendix*, Fig. S2). Ocean sources of terrestrial plastic deposition were important in coastal areas, including the west coast of North America, the Mediterranean region, and southern Australia (*SI Appendix*, Fig. S2). Dust and agricultural sources of plastic deposition were more important in northern Africa and Eurasia, while road sources were more important in heavily populated regions (*SI Appendix*, Fig. S4). More observations are required in all these locations that are modeled to have high concentrations in order to verify that the sources postulated here are correct.

Next, we considered our estimated net import and export of plastics from each ocean and land region (Fig. 4*C*). While the data we used to constrain the sources concentrated on the western United States, the largest source of plastics was hypothesized to be from Africa, followed by Asia, suggesting more work in these continents is vital. The total deposition of plastic to ocean surfaces from land sources was 13 $Gg \cdot y^{-1}$ and total terrestrial deposition from ocean sources was 22 $Gg \cdot y^{-1}$ (excluding coastal grid boxes). Because oceans dominated the atmospheric burden of plastics, most continents were net importers of plastic material, except for South America, which was neutral. Antarctica had the greatest imbalance as it has zero emissions of plastics and yet receives deposition of 3.4×10^{-5} $Gg \cdot y^{-1}$. Most other regions imported plastics from the ocean at a rate that was 4 to 9% of their emissions, considering only grid boxes away from the coastal regions.

As plastic aerosols have unusual shapes (e.g., long fibers), the spectrum of residence times of these particles and fibers in the atmosphere is not well known and needs to be studied. Here, we used three different size distributions that span the available sizes within the data (Fig. 2*A*). We estimated that atmospheric residence times ranged from 0.04 d (~1 h) to 6.5 d for the different sizes of plastic particles simulated here (*SI Appendix*, Table S4). The largest atmospheric source, the ocean, had the shortest residence time ranging from 0.1 to 1.7 d, with the mass-weighted mean lifetime being 0.10 d. Road sources ranged from 1 h to 2.9 d (mean: 0.62 d), while agriculture or population dust plastics had the longest atmospheric residence times ranging from 0.06 to 5.8 d and 0.07 to 6.5 d respectively (mean: 0.92 and 0.91 d, respectively). Since fine aerosols can travel between continents in just a few days (64–66), these data suggest that, under the right conditions, plastics can be transported across the major oceans and between continents, either in one trip or by resuspension over the oceans. More data on how these plastics will behave in the atmosphere in terms of their dry and wet deposition rates is needed to better constrain the residence times. Note that here we do not have data for microplastics smaller than 4 μm, and these difficult to measure particles need to be quantified as well.

We determined that, at present, microplastics make up less than 1% of the anthropogenic aerosol deposition over terrestrial environments but alarmingly already may make up greater than 50% [0 to 90%, 95% confidence limits] of the net anthropogenic atmospheric aerosol deposition over parts of the oceans downwind

of the major ocean plastic source, making up more than black carbon, organic carbon, sulfate, and agricultural dusts combined (*SI Appendix*, Fig. S5). This is not entirely surprising given that the observed percentage of plastics in all aerosol deposition in remote mountains sites ranged from 2 to 6% (average 4%) (23). A recent examination of plastic concentrations in agricultural soils found microplastics even in fields where biosolid and plastic mulch applications had not occurred (52). In addition, despite the large size of the microplastics and their short residence times, contemporary atmospheric surface concentrations over the ocean source regions may be as large as 5% of the mass of anthropogenic aerosols (*SI Appendix*, Fig. S5). While these concentrations remain low, they are unlikely to impact climate or radiative forcing, these findings underscore the role of atmospheric deposition in contributing plastics broadly across landscape types and their potential for re-emission to the atmosphere. Due to the ubiquity of microplastic deposition, it seems plausible that any and all dusts should contain microplastic pollution. In fact, Brahney et al. (23) showed strong positive relationships to contemporaneous dust deposition in wet deposition. Given this understanding, the global production of dust and the land-use activities that contribute to the destabilization of soils (67–70) also contribute to the global dispersion of plastic. Although smaller than the current total anthropogenic fine particle emissions (30 $Tg \cdot y^{-1}$), the current atmospheric source of microplastics is 8.6 [0 to 22] $Tg \cdot y^{-1}$, which is of the same order of magnitude as the current anthropogenic and biomass burning sources of black carbon aerosols to the atmosphere (10 $Tg \cdot y^{-1}$) (71–73). Industrial aerosol emissions should be decreasing in the next few decades (74), while microplastics could be increasing if unmitigated, suggesting that plastic aerosols could become more important in the coming years. These numbers are heavily dependent on the very uncertain ocean source, so more investigation of the ocean source and its potential growth is vital as the direct and indirect effect of plastic aerosols on the climate is not known.

One of the most compelling results to emerge from our synthesis of model and data are that re-emission sources dominate the atmospheric burden of plastics. This implies that the historical production of plastics is important for determining atmospheric plastic concentration and deposition. This result aligns with global plastic production and the fact that most polymer types can take decades or centuries to decompose to base elements (75, 76). In the meantime, they fragment into smaller and smaller pieces and become available for wind transport. Extrapolating from Geyer et al. (1) indicates that, in 2019, plastic production would have represented only 4% of total plastic production since 1950. Thus, the amount of microplastics in the environment available for atmospheric transport has grown to the point that it dwarfs primary annual emissions from urban centers. The fact that most continents were net importers of atmospheric plastics from the marine environment highlights the role of legacy plastics in contributing to the atmospheric burden of plastics and its eventual fallout. Removing plastics from the oceans might not only improve marine water quality but also significantly reduce the atmospheric redistribution of the microplastics (5).

Current deposition rates in terrestrial environments peak at above 10 $mg \cdot m^{-2} \cdot d^{-1}$ (Fig. 3*A*). Though future estimates are uncertain, using the high growth rate estimates from ref. 2 suggest that plastic deposition rates may increase to 100 $mg \cdot m^{-2} \cdot d^{-1}$ by 2050, which raises questions on the impact of accumulating plastics in the atmosphere on human health as well as wildland soils and waters. The inhalation of particles can be irritating to lung tissue and lead to serious diseases (45), but whether plastics are more or less toxic than other aerosols is not yet well understood (77). At present, we know very little about the effect of plastics concentrations in soils or waters and what threshold concentrations start to incur negative abiotic or biotic effects on ecosystem functioning. Although the addition of plastic mulch has shown short-term benefits for plant production, recent studies showed that plastic accumulation in soils ultimately has a negative effect on plant yield and nutrient availably (7, 8). Microplastics may even have the potential to accumulate in plants (78, 79). Our relative ignorance of the consequences despite rapidly rising plastic concentrations in our environment highlights the importance of improving plastic waste management (4) or, indeed, capturing ocean plastics and removing them from the system (80).

To better constrain the global plastic cycle, in particular the atmospheric limb, several knowledge and data gaps need to be filled. These include size-resolved temporal deposition data across diverse landscapes and specifically on continents where limited to no data exist (e.g., South America and Africa), more studies on prospective emission sources including marine, agricultural, and road emissions as they may differ by region, emissions from households and industries, and additional studies on the aerodynamics of plastic fibers, films, and particles. In situ atmospheric concentrations of microplastics and paleo studies including ice core data can improve our understanding of the temporal changes in microplastic transport, transport distances, and deposition rates.

Conclusion

In modeling the sources of plastic to the atmosphere, we show how the global plastic cycle is influenced more by historical plastic sources from mismanaged waste than emissions in the current year. In the western United States, roads and ocean sources contributed 84 and 11% of the modeled plastic deposition, while agricultural dusts and population sources contributed 5 and 0.4%, respectively. Oceans dominated plastic sources at the global scale, accounting for 99% of the deposition to oceans and 7% of the deposition to land surfaces away from coastal regions. Roads, agricultural dust, and dust sources near population centers were also important sources of deposition to terrestrial environments. Because marine sources dominated atmospheric loads, most terrestrial environments were net importers of plastics.

Though our modeling efforts have advanced our understanding of plastic movement through atmospheric reservoirs and provided key insights into the major sources of atmospheric plastics, our first study on the relative importance of different sources leads to more questions than it definitively answers. Specifically, how do rates of emissions from different sources vary by land use or technology? For example, do European roads emit more plastic than US roads due to polymer additions to asphalt binding agents? Or is population density a better predictor? How do agricultural soil microplastic concentrations vary between countries that use different practices? How do coastal sea spray emissions vary? Do changes in ocean circulation matter? In addition, key questions remain on the dominant size fractions found within the atmosphere, particularly those in the nanoplastic range. With respect to future emissions, changes in global waste management of plastics will influence emission rates from the key oceanic and terrestrial sources, but more information is needed on oceanic and terrestrial reservoir residence times. Finally, important questions remain on the potential impacts to the atmosphere and climate. Similar to other insoluble particles such as desert dust, do atmospheric microplastics act as cloud condensation or more likely ice nuclei? Additional data on in situ atmospheric microplastic concentrations as well as contemporary and historical deposition rates in space and time will further improve our understanding of the atmospheric limb of the plastic cycle.

Materials and Methods

Deposition Data. Deposition data from the western United States were collected at National Atmospheric Deposition Network stations over a 14-mo period using Aerochem Metrics model 31 wet/dry collectors fitted with Dry Sampling Units (81). Dry deposition data were collected at monthly intervals while wet deposition was collected at weekly intervals at 11 stations (listed in *SI Appendix*, Table S1). A total of 313 samples were counted for total microplastic abundance. The size and length of each particle and fiber were

determined. The minimum visible size was ~4 μm, and size distribution was skewed unimodal tapering toward the smaller size classes, suggesting the data captured the bulk of the plastic mass by size class. Mass deposition rates were determined based on the mean density and detailed analysis of the distribution of polymer sizes and volumes. See ref. 23 for more details.

Atmospheric Microplastics Transport Model. The CAM version 5 in Community Earth System Model (CESM) version 1.2.2 (82) was applied for computing the atmospheric transport of the microplastics. The model was run with 1° horizontal resolution for years 2015 through 2019, with the first year discarded for spin-up, forced with meteorological data from the Modern Era Retrospective Reanalysis for Research and Analysis, which represents a combination of observations and models for each 6-h time period (83). The default model includes aerosol representations of anthropogenic and natural aerosols, which interact through radiative and cloud processes with the physical climate (84). The default model includes sea spray and dust sources, which are prognostically calculated based on wind strength as well as soil moisture for dust sources (84, 85). The model output consisted of monthly and daily maps of source, concentrations, and wet and dry deposition of microplastic tracers, windblown dust, sea spray aerosols, and monthly average fields of other aerosols and meteorological quantities.

The microplastics were added to the model as insoluble aerosol tracer species with six different aerodynamic diameters in different bins (0.3, 2.5, 7, 15, 35, and 70 μm) using a separate aerosol framework (86), as these size bins are likely to be able to resolve the evolution of the size distribution due to differences in lifetimes of particles (e.g., ref. 87). These do not impact radiation or cloud formation but are subject to wet and dry deposition removal processes. Since the aerodynamic size of the plastics is very important for the atmospheric residence time but poorly understood for fibers and other asymmetric shapes (42, 43), and recognizing that there are suggestions that models may overestimate dry deposition rates for large asymmetric particles even for well-studied aerosols like dust (88), we use three different size assumptions for our model-data comparison, with our base case being the medium size (Fig. 2*A*). We assumed a density of 1 g · cm^{-3} for all particles. For each source, the source size distribution is tuned so that the average size distribution of deposition at the sites is matched for each of the three different sizes using the information from the observations for both the number and volume of the plastic particles and fibers.

We considered a number of possible microplastic emission sources including marine, road, dust, and population centers. In order to simulate the marine emission of microplastics with sea spray, we first estimated the distribution of microplastics in the ocean surface layer using the following method to reproduce a smooth field that reproduced the observations (8). As the microplastic particles in the ocean surface layer are lighter than the water, they accumulate in convergence zones with downward currents and slow velocities. We used the horizontal water velocity fields of the upmost ocean layer from the CESM Large Ensemble (89) transient simulations of the 20th century and computed a proxy for the plastic concentrations proportional to the flow convergence and inversely proportional to its velocity. This proxy was normalized to one and taken to power x = 10, which was determined by fitting to reproduce the dynamic variability of published measurements and modeling studies (3, 80, 90–94). The different ocean basins were further calibrated so that the cumulative microplastics for each basin matched the mean of the three estimates for each basin (22). The spatial distribution of microplastic concentrations in the upper ocean was held fixed, while the emissions were prognostically calculated at every time step as a function of this spatial distribution times the sea spray source and multiplied by a globally constant factor deduced from the observations, as described later.

Road tire and braking emissions come from an inventory (36) representing microplastics in fine, coarse, and larger aerosol size ranges based on road-miles driven and braking estimates using the Greenhouse gas–Air pollution Interactions and Synergies (http://gains.iiasa.ac.at/) model (73). The spatial distribution of this source was fixed to the sum of tire and braking emissions and held constant in time and multiplied by a global constant deduced from the observations.

Simulations of agricultural sources of microplastics assumed that all crop areas have the same soil fraction of microplastics and simply apply the fraction of the grid box that is a crop for 2005 based on land use and land cover datasets for the Climate Model Intercomparison Project for the CESM (95). This crop area factor is multiplied by the prognostic dust generation within the model, which depends on low values of leaf area index (<0.3 m^2 · m^{-2}) and soil moisture, as well as strong winds, to generate dust and thus microplastics in dust (85).

Population density map from Gridded Population of the World version 4 (96) for 2015 at 15 arc minutes resolution was used as a proxy for direct emissions from households (e.g., dryer vents), businesses, construction work, and waste management. This source was assumed to be constant in time (referred to as population source). To estimate the plastics generated downwind from population sources near arid regions (referred to as population-dust source), the wet and dry deposition maps from this source were added together and overlain with the natural weather and land-cover–dependent windblown dust emissions from the model to simulate the re-emission of the deposited particles from dry erodible landscapes.

Modeling is done for 2015 through 2019 and comparisons are made for the exact time period of the observations for the optimal estimation (97). For the mean distribution, to account for interannual variability, 3 y of simulations are averaged and shown.

Optimal Estimation of Atmospheric Microplastics Source. The atmospheric plastic module produces the spatial and temporal variability in the deposition to be compared against observations for the exact same time period. For each source, one global tuning number is estimated using optimal estimation methods to best fit the observations of deposition. For each model source (ocean, road tire and braking (referred to as roads), agricultural dust, population dust, and population) the deposition (dry or wet) is calculated at each site over the observation time period separately for the weekly to monthly dry (n = 103) and approximately weekly wet (n = 213) observations at each of 11 sites described in ref. 23 and listed in *SI Appendix*, Table S1. The source strength for each source (S_i) is calculated to minimize the following cost function, which also represents a χ^2 goodness of fit (98).

$$\chi^2 = \sum_j \left[\frac{\left(y_{model,j} - y_{obs,j}\right)}{\sigma_j} \right]^2 + P, \quad [1]$$

where $y_{obs,j}$ are the 316 observations, and $y_{model,j}$ is found using the following equation:

$$y_{model,j} = \sum_i S_i * R_{i,j},$$

where $R_{i,j}$ is the modeled relationship between each source (i) and the deposition at each site (j). P represents a penalty which is assessed if any of the sources become negative. The magnitude of this is set to force all the estimations to result in positive values. The σ_j is the model-observational error or uncertainty in each observation when compared against the model. This will be the sum of direct observational error, in addition to the error in the model's ability to represent accurately the observation. The observational error had a mean of 1.3 fibers in the process blanks for the wet deposition. This translates to a mean error of 20% for wet deposition and 1.6% for dry deposition. In addition, the model is not able to perfectly represent the deposition to a particular location, especially in complex terrain. Previous estimates have suggested for natural coarse mode aerosols, such as dust, that model-data deposition comparisons may be off by one order of magnitude (99). Here, we estimate our errors using model-data comparisons of dust and sodium (in wet deposition), which indicate an error of ~50% (*SI Appendix*, Table S2). We also have a constraint that the goodness of fit (χ^2) should be about the same value as our number of observations (n = 313) (98) and thus for the comparison using all values, we needed to increase our errors by 50% to meet this criteria (therefore 75% + [30% or 2.4% depending on whether wet or dry deposition]).

The minimum in the cost function (χ^2) was found using a global search across the viable values of the source strengths (between 0 and a value that would provide all the required plastics at the deposition sites) combined with the fminsearch in matlab. This was done sequentially across all five sources with 30 values for each source (thus 30^5 calculations to initialize the global search). In addition, some of the values were small, so this was repeated using a smaller areal range (0 to 0.1 for the small sources) to better define the confidence levels. The 95% confidence levels for each of the source strengths can be estimated by the values of the source strength which produce χ^2 values equal to the minimum value plus 4 (98) if the errors are Gaussian. Although our errors are not strictly Gaussian, we report these values as an estimate of the source strengths that are within our 95% CIs. We obtain the following cost function (χ^2) for the three sizes: 376.7, 375.4, and 432.5 for the large, medium, and small particles (shown in Fig. 2*A*). The strength of each source for the base case by bin, using the optimal estimation, is shown in *SI Appendix*, Table S3.

We conduct two additional sensitivity studies using different subsets of our data to understand the importance of the temporal and spatial

resolution of our deposition data. First, instead of using 313 data points across 11 sites, we average the dry and wet deposition at each site and use that value to conduct the optimization in Eq. **1** using only 11 values instead of 313. For this sensitivity study, we used the original 50% error estimate, as the (χ^2) were of the same order as the number of sites in that analysis. This study shows that having temporal resolution reduces the range of confidence limits (cyan colors in Fig. 2*B*). Our second sensitivity study explores the value of each additional site and tests whether one site is overly driving the analysis. Here, each of the 11 sites is excluded from the analysis, resulting in a large range in the CIs (green colors in Fig. 2*B*).

In addition, we conduct an additional sensitivity study where we include the a priori information about the source strength of the road and braking source using a Bayesian approach (described in more detail in the *SI Appendix*). We also conduct a sensitivity study where we use a different estimate of the spatial distribution of the ocean source based on a different interpolation of the observations (22) with more details (results described in more detail in the *SI Appendix*). Neither of these sensitivity studies were as important as which data were included (described above).

Data Availability. Deposition data have been deposited in the Environmental System Science Data Infrastructure for a Virtual Ecosystem, https://data.ess-dive.lbl.gov/view/doi:10.15485/1773176 (see also the supplemental materials in ref. 23). Model output is available in Cornell eCommons at https://doi.org/10.7298/4mdh-4e97.

ACKNOWLEDGMENTS. This research was supported by Agricultural Experimental Station Research Grants UTA01421 and UTA01384 and approved as journal paper No. 9442, NSF Awards 1926559 and 2011910, and a United States Department of Agriculture Forest Service Agreement to J.B. N.M. and M.P. acknowledge support from the Cornell Atkinson Center for Sustainability, the NSF's National Center for Atmospheric Research Computing facilities, and NSF Award CCF-1522054; they were also supported by the Academy of Finland (project number 322532). H.M. was supported by the Ministry of Education, Culture, Sports, Science, and Technology, Japan Society for the Promotion of Science (MEXT/JSPS) KAKENHI Grants JP17H04709 and JP19H05699, the MEXT Arctic Challenge for Sustainability Grants (ArCS, Grant JPMXD1300000000) and ArCS-II (Grant JPMXD1420318865) projects, and by the Environment Research and Technology Development Fund 2-1703 (Grant JPMEERF20172003) and 2-2003 (Grant JPMEERF20202003) of the Environmental Restoration and Conservation Agency. We thank Sagar Rathod for assistance to N.M.

1. R. Geyer, J. R. Jambeck, K. L. Law, Production, use, and fate of all plastics ever made. *Sci. Adv.* **3**, e1700782 (2017).
2. J. R. Jambeck *et al*., Plastic waste inputs from land into the ocean. *Science* **347**, 768–771 (2015).
3. M. Eriksen *et al*., Plastic pollution in the world's oceans: More than 5 trillion plastic pieces weighing over 250,000 tons afloat at sea. *PLoS One* **9**, e111913 (2014).
4. L. Lebreton, A. Andrady, Future scenarios of global plastic waste generation and disposal. *Palgrave Commun.* **5**, 1–11 (2019).
5. W. W. Y. Lau *et al*., Evaluating scenarios toward zero plastic pollution. *Science* **369**, 1455–1461 (2020).
6. S. B. Borrelle *et al*., Predicted growth in plastic waste exceeds efforts to mitigate plastic pollution. *Science* **369**, 1515–1518 (2020).
7. D. Zhang *et al*., Plastic pollution in croplands threatens long-term food security. *Glob. Change Biol.* **26**, 3356–3367 (2020).
8. J. Wang *et al*., Effects of plastic film residues on occurrence of phthalates and microbial activity in soils. *Chemosphere* **151**, 171–177 (2016).
9. Y. Huang *et al*., LDPE microplastic films alter microbial community composition and enzymatic activities in soil. *Environ. Pollut.* **254**, 112983 (2019).
10. E. L. Ng *et al*., Microplastic pollution alters forest soil microbiome. *J. Hazard. Mater.* **409**, 124606 (2021).
11. M. T. Kettner, K. Rojas-Jimenez, S. Oberbeckmann, M. Labrenz, H. P. Grossart, Microplastics alter composition of fungal communities in aquatic ecosystems. *Environ. Microbiol.* **19**, 4447–4459 (2017).
12. S. Oberbeckmann, M. G. J. Loeder, G. Gerdts, A. M. Osborn, Spatial and seasonal variation in diversity and structure of microbial biofilms on marine plastics in Northern European waters. *FEMS Microbiol. Ecol.* **90**, 478–492 (2014).
13. W. Wang, H. Gao, S. Jin, R. Li, G. Na, The ecotoxicological effects of microplastics on aquatic food web, from primary producer to human: A review. *Ecotoxicol. Environ. Saf.* **173**, 110–117 (2019).
14. Y. Chae, Y.-J. An, Nanoplastic ingestion induces behavioral disorders in terrestrial snails: Trophic transfer effects via vascular plants. *Environ. Sci. Nano* **7**, 975–983 (2020).
15. C. M. Rochman, E. Hoh, T. Kurobe, S. J. Teh, Ingested plastic transfers hazardous chemicals to fish and induces hepatic stress. *Sci. Rep.* **3**, 3263 (2013).
16. L. M. Ziccardi, A. Edgington, K. Hentz, K. J. Kulacki, S. Kane Driscoll, Microplastics as vectors for bioaccumulation of hydrophobic organic chemicals in the marine environment: A state-of-the-science review. *Environ. Toxicol. Chem.* **35**, 1667–1676 (2016).
17. N. Hirt, M. Body-Malapel, Immunotoxicity and intestinal effects of nano- and microplastics: A review of the literature. *Part. Fibre Toxicol.* **17**, 57 (2020).
18. L. Rubio, R. Marcos, A. Hernández, Potential adverse health effects of ingested micro- and nanoplastics on humans. Lessons learned from *in vivo* and *in vitro* mammalian models. *J. Toxicol. Environ. Health B Crit. Rev.* **23**, 51–68 (2020).
19. C. M. Rochman, T. Hoellein, The global odyssey of plastic pollution. *Science* **368**, 1184–1185 (2020).
20. M. S. Bank, S. V Hansson, The plastic cycle: A novel and holistic paradigm for the anthropocene. *Environ. Sci. Technol.* **53**, 7177–7179 (2019).
21. A. A. Horton, S. J. Dixon, Microplastics: An introduction to environmental transport processes. *Wiley Interdiscip. Rev. Water* **5**, e1268 (2018).
22. E. Van Sebille, C. Spathi, A. Gilbert, The ocean plastic pollution challenge: Towards solutions in the UK. *Grant. Brief. Pap* **19**, 1–16 (2016).
23. J. Brahney, M. Hallerud, E. Heim, M. Hahnenberger, S. Sukumaran, Plastic rain in protected areas of the United States. *Science* **368**, 1257–1260 (2020).
24. S. Allen *et al*., Atmospheric transport and deposition of microplastics in a remote mountain catchment. *Nat. Geosci.* **12**, 339 (2019).
25. M. Bergmann *et al*., White and wonderful? Microplastics prevail in snow from the Alps to the Arctic. *Sci. Adv.* **5**, eaax1157 (2019).
26. R. Dris *et al*., A first overview of textile fibers, including microplastics, in indoor and outdoor environments. *Environ. Pollut.* **221**, 453–458 (2017).
27. S. L. Wright, J. Ulke, A. Font, K. L. A. Chan, F. J. Kelly, Atmospheric microplastic deposition in an urban environment and an evaluation of transport. *Environ. Int.* **136**, 105411 (2020).
28. L. Cai *et al*., Characteristic of microplastics in the atmospheric fallout from Dongguan city, China: Preliminary research and first evidence. *Environ. Sci. Pollut. Res. Int.* **24**, 24928–24935 (2017).
29. R. Dris *et al*., Microplastic contamination in an urban area: A case study in greater Paris. *Environ. Chem.* **12**, 592–599 (2015).
30. J. H. Seinfeld, S. N. Pandis, *Atmospheric Chemistry and Physics: From Air Pollution to Climate Change* (John Wiley & Sons, 2016).
31. S. Allen *et al*., Examination of the ocean as a source for atmospheric microplastics. *PLoS One* **15**, e0232746 (2020).
32. G. C. Cornwell, *et al*., Ejection of dust from the ocean as a potential source of marine ice nucleating particles. *J. Geophys. Res. Atmos.* **125**, e2020JD033073 (2020).
33. S. Wagner *et al*., Tire wear particles in the aquatic environment–A review on generation, analysis, occurrence, fate and effects. *Water Res.* **139**, 83–100 (2018).
34. F. Sommer *et al*., Tire abrasion as a major source of microplastics in the environment. *Aerosol Air Qual. Res.* **18**, 2014–2028 (2018).
35. C. Vogelsang, *et al*., Microplastics in road dust–Characteristics, pathways and measures. https://www.miljodirektoratet.no/globalassets/publikasjoner/M959/M959.pdf. Accessed 29 March 2021.
36. N. Evangeliou *et al*., Atmospheric transport is a major pathway of microplastics to remote regions. *Nat. Commun.* **11**, 3381 (2020).
37. S. I. Torri, R. S. Corrêa, G. Renella, L. Perelomov, A. Valdecantos, Biosolids soil application: Agronomic and environmental implications 2013. *Appl. Environ. Soil Sci.* **2014**, 1–3 (2014).
38. L. Nizzetto, M. Futter, S. Langaas, Are agricultural soils dumps for microplastics of urban origin? *Environ. Sci. Technol.* **50**, 10777–10779 (2016).
39. F. Murphy, C. Ewins, F. Carbonnier, B. Quinn, Wastewater treatment works (WwTW) as a source of microplastics in the aquatic environment. *Environ. Sci. Technol.* **50**, 5800–5808 (2016).
40. M. Lalitha, V. K. Thilagam, N. Balakrishnan, M. Mansour, Effect of plastic mulch on soil properties and crop growth-A review. *Agric. Rev. (Karnal)* **31**, 145–149 (2010).
41. R. B. Neale *et al*., The mean climate of the Community Atmosphere Model (CAM4) in forced SST and fully coupled experiments. *J. Clim.* **26**, 5150–5168 (2013).
42. A. Heymsfield, Ice crystal terminal velocities. *J. Atmos. Sci.* **29**, 1348–1357 (1972).
43. P. Ginoux, Effects of nonsphericity on mineral dust modeling. *J. Geophys. Res. Atmos.* **108**, 4052 (2003).
44. N. Mahowald *et al*., Aerosol impacts on climate and biogeochemistry. *Annu. Rev. Environ. Resour.* **36**, 47–74 (2011).
45. A. Churg, M. Brauer, Human lung parenchyma retains PM2.5. *Am. J. Respir. Crit. Care Med.* **155**, 2109–2111 (1997).
46. J. F. Kok *et al*., Smaller desert dust cooling effect estimated from analysis of dust size and abundance. *Nat. Geosci.* **10**, 274–278 (2017).
47. J. Neff, M. P. Reynolds, S. Munson, D. Fernandez, J. Belnap, The role of dust storms in total amtospheric particle concentration at two sites in the western U.S. *J. Geophys. Res.* **118**, 1–12 (2013).
48. K. Magnusson *et al*., "Swedish sources and pathways for microplastics to the marine environment. A review of existing data" (Rep. C183, IVL, Stockholm, Sweden, 2016).
49. Y. Shao *et al*., Dust cycle: An emerging core theme in Earth system science. *Aeolian Res.* **2**, 181–204 (2011).
50. E. D. Nilsson *et al*., Turbulent aerosol fluxes over the Arctic Ocean: 2. Wind-driven sources from the sea. *J. Geophys. Res. Atmos.* **106**, 32139–32154 (2001).
51. P. Ginoux, J. M. Prospero, T. E. Gill, N. C. Hsu, M. Zhao, Global-scale attribution of anthropogenic and natural dust sources and their emission rates based on MODIS Deep Blue aerosol products. *Rev. Geophys.* **50**, RG3005 (2012).
52. J. Crossman, R. R. Hurley, M. Futter, L. Nizzetto, Transfer and transport of microplastics from biosolids to agricultural soils and the wider environment. *Sci. Total Environ.* **724**, 138334 (2020).
53. G. S. Zhang, Y. F. Liu, The distribution of microplastics in soil aggregate fractions in southwestern China. *Sci. Total Environ.* **642**, 12–20 (2018).
54. E. K. Liu, W. Q. He, C. R. Yan, 'White revolution' to 'white pollution'—agricultural plastic film mulch in China. *Environ. Res. Lett.* **9**, 91001 (2014).

55. F. Corradini *et al*., Evidence of microplastic accumulation in agricultural soils from sewage sludge disposal. *Sci. Total Environ.* **671**, 411–420 (2019).
56. M. Rezaei, M. J. P. M. Riksen, E. Sirjani, A. Sameni, V. Geissen, Wind erosion as a driver for transport of light density microplastics. *Sci. Total Environ.* **669**, 273–281 (2019).
57. S. Hann *et al*., Investigating options for reducing releases in the aquatic environment of microplastics emitted by (but not intentionally added in) products. https://bmbf-plastik.de/sites/default/files/2018-04/microplastics_final_report_v5_full.pdf. Accessed 29 March 2021.
58. J. Gavigan, T. Kefela, I. Macadam-Somer, S. Suh, R. Geyer, Synthetic microfiber emissions to land rival those to waterbodies and are growing. *PLoS One* **15**, e0237839 (2020).
59. U. Pirc, M. Vidmar, A. Mozer, A. Kržan, Emissions of microplastic fibers from microfiber fleece during domestic washing. *Environ. Sci. Pollut. Res. Int.* **23**, 22206–22211 (2016).
60. D. Kawecki, B. Nowack, Polymer-specific modeling of the environmental emissions of seven commodity plastics as macro-and microplastics. *Environ. Sci. Technol.* **53**, 9664–9676 (2019).
61. S. Dehghani, F. Moore, R. Akhbarizadeh, Microplastic pollution in deposited urban dust, Tehran metropolis, Iran. *Environ. Sci. Pollut. Res. Int.* **24**, 20360–20371 (2017).
62. M. Klein, E. K. Fischer, Microplastic abundance in atmospheric deposition within the Metropolitan area of Hamburg, Germany. *Sci. Total Environ.* **685**, 96–103 (2019).
63. G. Suaria *et al*., Microfibers in oceanic surface waters: A global characterization. *Sci. Adv.* **6**, eaay8493 (2020).
64. A. Stohl, S. Eckhardt, C. Forster, P. James, N. Spichtinger, On the pathways and timescales of intercontinental air pollution transport. *J. Geophys. Res. Atmos.* **107**, ACH 6-1–ACH 6-17 (2002).
65. M. Prank, S. C. Kenaley, G. C. Bergstrom, M. Acevedo, N. M. Mahowald, Climate change impacts the spread potential of wheat stem rust, a significant crop disease. *Environ. Res. Lett.* **14**, 124053 (2019).
66. D. Griffin, C. Kellogg, E. Shinn, Dust in the wind: Long range transport of dust in the Atmosphere and its implications for global public and ecosystem health. *Glob. Change Hum. Health* **2**, 20–33 (2001).
67. J. C. Neff *et al*., Increasing eolian dust deposition in the western United States linked to human activity. *Nat. Geosci.* **1**, 189–195 (2008).
68. I. Tegen, M. Werner, S. P. Harrison, K. E. Kohfeld, Relative importance of climate and land use in determining present and future global soil dust emission. *Geophys. Res. Lett.* **31**, L05105 (2004).
69. N. M. Mahowald, G. D. R. Rivera, C. Luo, Comment on "Relative importance of climate and land use in determining present and future global soil dust emission" by I. Tegen et al. *Geophys. Res. Lett.* **31**, L24105 (2004).
70. J. P. Field *et al*., The ecology of dust. *Front. Ecol. Environ.* **8**, 423–430 (2009).
71. M. Gidden *et al*., Global emissions pathways under different socioeconomic scenarios for use in CMIP6: A dataset of harmonized emissions trajectories through the end of the century. *Geosci. Model Dev. Discuss.* **12**, 1443–1475 (2019).
72. R. M. Hoesly *et al*., Historical (1750-2014) anthropogenic emissions of reactive gases and aerosols from the Community Emission Data System (CEDS). *Geosci. Model Dev.* **11**, 369–408 (2018).
73. Z. Klimont *et al*., Global anthropogenic emissions of particulate matter including black carbon. *Atmos. Chem. Phys. Discuss.* **17**, 8681–8723 (2017).
74. K. Riahi *et al*., The shared socioeconomic pathways and their energy, land use, and greenhouse gas emissions implications: An overview. *Glob. Environ. Change* **42**, 153–168 (2017).
75. H. K. Webb, J. Arnott, R. J. Crawford, E. P. Ivanova, Plastic degradation and its environmental implications with special reference to poly (ethylene terephthalate). *Polymers (Basel)* **5**, 1–18 (2013).
76. R.-J. Müller, I. Kleeberg, W.-D. Deckwer, Biodegradation of polyesters containing aromatic constituents. *J. Biotechnol.* **86**, 87–95 (2001).
77. S. L. Wright, F. J. Kelly, Plastic and human health: A micro issue? *Environ. Sci. Technol.* **51**, 6634–6647 (2017).
78. M. C. Rillig, Plastic and plants. *Nat. Sustain.* **3**, 887–888 (2020).
79. L. Li *et al*., Effective uptake of submicrometre plastics by crop plants via a crack-entry mode. *Nat. Sustain.* **3**, 1–9 (2020).
80. P. Sherman, E. Van Sebille, Modeling marine surface microplastic transport to assess optimal removal locations. *Environ. Res. Lett.* **11**, 14006 (2016).
81. J. Brahney *et al*., A new sampler for the collection and retrieval of dry dust deposition. *Aeolian Res.* **45**, 100600 (2020).
82. J. W. Hurrell *et al*., The community earth system model: A framework for collaborative research. *Bull. Am. Meteorol. Soc.* **94**, 1339–1360 (2013).
83. R. Gelaro *et al*., The modern-era retrospective analysis for research and applications, version 2 (MERRA-2). *J. Clim.* **30**, 5419–5454 (2017).
84. X. Liu *et al*., Towards a minimal representation of aerosol direct and indirect effects: Model description and evaluation. *Geosci. Model Dev.* **5**, 709–735 (2012).
85. S. Albani *et al*., Improved dust representation in the community Atmosphere model. *J. Adv. Model. Earth Syst.* **6**, 541–570 (2014).
86. H. Matsui, N. Mahowald, Development of a global aerosol model using a two-dimensional sectional method: 2. Evaluation and sensitivity simulations. *J. Adv. Model. Earth Syst.* **9**, 1887–1920 (2017).
87. N. Mahowald *et al*., The size distribution of desert dust aerosols and its impact on the Earth system. *Aeolian Res.* **15**, 53–71 (2014).
88. C. L. Ryder *et al*., Coarse and giant particles are ubiquitous in Saharan dust export regions and are radiatively significant over the Sahara. *Atmos. Chem. Phys.* **19**, 15353–15376 (2019).
89. J. E. Kay *et al*., The community Earth System model (CESM) large ensemble project: A community resource for studying climate change in the presence of internal climate variability. *Bull. Am. Meteorol. Soc.* **96**, 1333–1349 (2015).
90. A. Cózar *et al*., Plastic debris in the open ocean. *Proc. Natl. Acad. Sci. U.S.A.* **111**, 10239–10244 (2014).
91. E. Van Sebille *et al*., A global inventory of small floating plastic debris. *Environ. Res. Lett.* **10**, 124006 (2015).
92. E. Van Sebille, M. H. England, G. Froyland, Origin, dynamics and evolution of ocean garbage patches from observed surface drifters. *Environ. Res. Lett.* **7**, 044040 (2012).
93. L. C. M. Lebreton, S. D. Greer, J. C. Borrero, Numerical modelling of floating debris in the world's oceans. *Mar. Pollut. Bull.* **64**, 653–661 (2012).
94. N. Maximenko, J. Hafner, P. Niiler, Pathways of marine debris derived from trajectories of Lagrangian drifters. *Mar. Pollut. Bull.* **65**, 51–62 (2012).
95. P. J. Lawrence *et al*., Simulating the biogeochemical and biogeophysical impacts of transient land cover change and wood harvest in the Community Climate System Model (CCSM4) from 1850 to 2100. *J. Clim.* **25**, 3071–3095 (2012).
96. Center for International Earth Science Information Network, Data from "Gridded population of the world, Version 4 (GPWv4): Population density, Revision 11." NASA Socioeconomic Data and Applications Center (SEDAC). https://sedac.ciesin.columbia.edu/data/set/gpw-v4-population-density-rev11. Accessed 1 October 2020.
97. Computational and Information Systems Laboratory, Cheyenne: HPE/SGI ICE XA System (University Community Computing). https://doi.org/10.5065/D6RX99HX. Accessed 7 January 2021.
98. W. H. Press, S. A. Teukolsky, W. T. Vetterling, B. P. Flannery, *Numerical Recipes: The Art of Scientific Computing* (Cambridge University Press, 3rd Ed., 2007).
99. N. M. Mahowald *et al*., Atmospheric global dust cycle and iron inputs to the ocean. *Global Biogeochem. Cycles* **19**, GB4025 (2005).